MULTI-OBJECTIVE OPTIMIZATION TECHNIQUE TO OPTIMIZE THE PROCESS PARAMETERS OF EDM FOR AL ALLOYS USING TAGUCHI WITH GRA AND TOPSIS METHOD

B. Gugulothu[1,*], K. Srividya[2], D. B. Prakash[3], N. Dhasarathan[4], K. Bharadwaja[5], S. Karumuri[6]

[1]Saudi Electrical Services Polytechnic, Ras Tanura, Saudi Arabia
[2]Department of Mechanical Engineering, P V P Siddhartha Institute of Technology, Kanuru, Vijayawada, India
[3]Department of Mechanical Engineering, Swarnandhra College of Engineering & Technology, Sitharamapuram, India
[4]Department of ECE, Sri Venkateshwara College of Engineering, Bengaluru, India
[5]Department of Mechanical Engineering, Mallareddy (MR) Deemed to be University, secunderabad, India
[6]Department of Mechanical Engineering, Saveetha School of Engineering, SIMATS, Saveetha University, Tamil Nadu, India
*Corresponding author's e-mail address: b_gugulothu@sesp.edu.sa

ABSTRACT

Electrical Discharge Machining (EDM) is a non-traditional machining process which is employed to make complex products from hard materials. The machining efficiency and surface integrity are influenced by the selection of parameters. In this research, datasets were collected from earlier experimental research works on EDM process of AL alloy to evaluate machining performance. The input parameters are: pulse-on time, pulse-off time, discharge current, gap voltage, flushing pressure, and tool rotational speed and the output responses: material removal rate (MRR), tool wear rate (TWR), surface roughness (SRS), recast layer (RLR), and microhardness (MHS) were considered. MINITAB software was utilized to identify the most significant factors affecting responses through signal-to-noise analysis. For multi-objective optimization, the Taguchi method was integrated with Grey Relational Analysis (GRA) and Technique for Order Preference by Similarity to Ideal Solution (TOPSIS). From the results, GRA identified optimal parameters of discharge current of 11 A, pulse-on time of 75 µs, pulse-off time of 25 µs, gap voltage of 50 V, flushing pressure of 0.4 MPa, and tool speed of 600 rpm, yielding the highest productivity with MRR of 4.76 g/min, moderate TWR of 0.478 g/min. In contrast, TOPSIS suggested a discharge current of 7 A, pulse-on time of 175 µs, pulse-off time of 90 µs, gap voltage of 40 V, a flushing pressure of 0.5 MPa, and a tool speed of 900 rpm, which produced superior surface quality with a lower SRS of 7.34 µm, reduced RLR of 19.6 µm, higher MHS of 120.9 HV and a reduced MRR of 0.78 g/min. Both optimal results were validated using an Adaptive Neuro-Fuzzy Inference System (ANFIS) model, confirming accurate prediction of EDM responses. This study demonstrates that GRA is more suitable for productivity-focused applications, whereas TOPSIS is advantageous when surface integrity and hardness are critical, offering a robust decision-making framework for EDM optimization.

KEYWORDS: electrical discharge machining, Taguchi method, Grey Relational Analysis (GRA), TOPSIS optimization, ANFIS prediction model

1. INTRODUCTION

Many researchers have made significant contributions to the development and machining of composite materials, leading to the creation of lightweight, high-strength, and high-toughness materials essential in industries like aerospace, automotive, and nuclear. As manufacturing demands grow for materials with superior strength, hardness, and toughness, traditional machining methods struggle to effectively process these advanced materials. The combination of lightness, hardness, and toughness in modern materials often presents significant challenges during machining. As a result, non-conventional machining methods such as ECM, USM, EDM, and

Date of submission/acceptance: 07.09.2025/15.12.2025
https://doi.org/10.35219/awet.2025.11

newly developed hybrid techniques have emerged as viable solutions for processing materials that are difficult to machine.

EDM is a distinctive manufacturing technique employed to shape geometrically intricate and robust materials. This technique is categorised as a thermal machinability method due to its utilisation of electricity as an energy source. The machining performance does not influence the stiffness, hardness, or strength of the material being machined. On the other hand, the melting temperature and thermal conductivity of the material affect the machinability performance [1-3].

A significant quantity of thermal energy is focused in the minute discharge channel, with temperatures potentially reaching 10,000 °C, while pressure experiences abrupt fluctuations during the EDM process. Material removal in electric discharge machining occurs by electric heating during the discharge process, with the material's conductivity and thermal characteristics significantly influencing its machinability. In addition, it is particularly suitable for machining a workpiece with a complex surface, because the tool electrode shape can be copied to the workpiece [4-6].

The efficiency and precision of the EDM process are strongly influenced by the selection and optimization of various process parameters and These parameters are critical in determining MRR, TWR, surface finish, and the overall effectiveness of the machining process. Recent studies have shown that careful optimization of these parameters can significantly improve the machining performance, particularly for Al alloys, which are often challenging to machine due to their tendency to form a recast layer during EDM.

Various optimization techniques have been developed and applied to enhance EDM performance. For instance, the Taguchi method has been employed for optimizing process parameters because its simplicity in minimizing variation. Many authors used different optimization techniques such as Taguchi [7], RSM [8], GA [9], GRA [10], ANN [11] and ANFIS [12] for increasing the MRR and reducing Surface roughness on al alloys. This work presented an innovative approach by combining Taguchi method with GRA and TOPSIS to optimize EDM process parameters for aluminium alloys. This integration enables multi-response optimization, providing a thorough analysis of machining performance. Furthermore, ANFIS is utilized to accurately predict experimental results, leveraging the optimal parameters obtained from GRA and TOPSIS to enhance prediction accuracy. Figure 1 shows the flow chart of this work.

2. DATASET COLLECTION

The present dataset was collected from previous works [14-19]. According to the previous studies, the experimental factors considered include pulse-on time, gap voltage, discharge current, pulse-off time, flushing pressure, and tool rotational speed.

The input parameters and their levels were shown in table 1 and table 2 showed the combination of parameters generated using a Taguchi L27 orthogonal array design of experiments for EDM of aluminium alloy. The corresponding responses measured were MRR, tool wear rate (TWR), surface roughness (SRS), recast layer (RLR), and microhardness (MHS) of the machined surface and their results were displayed in table 3.

In the present work, optimal parameter settings for each response were determined using Minitab, while multi-objective optimization was carried out through GRA and TOPSIS to identify the best compromise parameters also aiming to maximize MRR and hardness and minimizing TWR, recast layer thickness, and Ra. Furthermore, ANFIS model was developed to predict the experimental dataset and validate the optimization results.

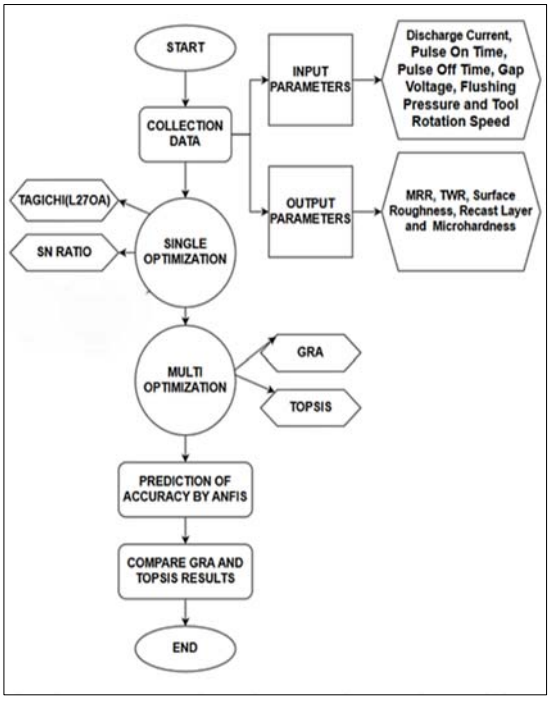

Fig. 1. Flow process of the EDM work

Table 1. Input parameters and levels

Sample	Parameters	Unit	Level -1	Level -2	Level -3
1	Ip	A	3	7	11
2	Ton	µs	75	175	275
3	Toff	µs	25	50	90
4	Vg	V	30	40	50
5	Fp	MPa	0.2	0.4	0.6
6	Tr	RPM	300	600	90

Table 2. Input parameters as per L27 orthogonal array

Experiment	Discharge current, Ip [A]	Pulse on time, Ton [µs]	Pulse off time, Toff [µs]	Gap voltage, Vg [V]	Flushing pressure, Fp [MPa]	Tool rotation speed, Tr [rpm]
1	7	75	25	40	0.2	300
2	11	75	25	50	0.2	300
3	3	175	25	30	0.2	300
4	7	175	25	40	0.2	300
5	11	175	25	50	0.2	300
6	3	275	25	30	0.2	300
7	7	275	25	40	0.2	300
8	11	275	25	50	0.4	300
9	3	75	50	30	0.4	600
10	7	75	50	40	0.4	600
11	11	75	50	50	0.4	600
12	3	175	50	30	0.4	600
13	7	175	50	40	0.4	600
14	11	175	50	50	0.4	600
15	3	275	50	30	0.4	600
16	7	275	50	40	0.6	600
17	11	275	50	50	0.6	600
18	3	75	90	30	0.6	900
19	7	75	90	40	0.6	900
20	11	75	90	50	0.6	900
21	3	175	90	30	0.6	900
22	7	175	90	40	0.6	900
23	11	175	90	50	0.6	900
24	3	275	90	30	0.2	900
25	7	275	90	40	0.2	900
26	11	275	90	50	0.2	900
27	3	75	25	30	0.2	300

Table 3. Output parameters of EDM work

Experiment	MRR [g/min]	TWR [g/min]	Surface roughness, Ra [µm]	Recast layer [µm]	Microhardness [HV]
1	1.94	0.42	6.06	37.8	98.3
2	4.76	0.48	9.23	20.5	86.2
3	3.69	0.05	1.07	4.8	103.2
4	3.03	0.49	2.12	19.4	92.9
5	0.86	0.14	0.64	20.2	154.4
6	0.86	0.06	3.39	44.1	144.6
7	0.38	0.76	4.01	38.6	130.7
8	4.34	0.77	2.86	53.4	149.7
9	3.05	0.65	8.32	28.9	144.3
10	3.57	0.25	3.7	8.1	94.9
11	0.20	0.09	2.95	43.1	151.4
12	4.85	0.55	5.52	45.9	123.1
13	4.18	0.36	1.58	34.1	144.6
14	1.14	0.11	8.06	46.5	151.7
15	0.99	0.40	0.93	30.1	105.4
16	1.00	0.04	9.87	31.8	88.8
17	1.59	0.73	7.77	26.2	98.2
18	1.53	0.26	8.19	2.9	148.9
19	1.08	0.72	8.66	45.6	155.4
20	2.22	0.53	0.25	7.4	145.4

Experiment	MRR [g/min]	TWR [g/min]	Surface roughness, Ra [µm]	Recast layer [µm]	Microhardness [HV]
21	3.10	0.42	7.13	38.6	80.6
22	0.78	0.44	7.34	19.6	120.9
23	2.33	0.62	3.71	15.7	89.6
24	1.90	0.78	0.93	54.6	97.8
25	1.53	0.16	7.76	31.0	113.4
26	3.95	0.75	1.34	25.2	107
27	2.67	0.21	2.15	2.5	114.2

3. TAGUCHI METHOD

In this work, for the evaluation of performance characteristics, SN ratio was applied: equation (1) was typically used for *the* larger-the-better response, whereas equation (2) was applied for the *smaller-the-better* response [20].

$$\mathrm{SN_{LB}} = -10\log_{10}\left(\frac{1}{n}\sum_{i=1}^{n}\frac{1}{y_i^2}\right) \quad (1)$$

$$\mathrm{SN_{SB}} = -10\log_{10}\left(\frac{1}{n}\sum_{i=1}^{n}y_i^2\right) \quad (2)$$

4. GRA TECHNIQUE

It involved several stages, beginning with the normalization of response data. This normalization step applies distinct criteria based on the nature of each response variable. The multi optimization approach was designed to increase MRR and micro hardness reducing Surface Roughness, TWR and Recast Layer. Accordingly, eqn (3) and eqn (4) employed for "larger-is-better" and "smaller-is-better" for normalization in GRA.

Step 1: *Normalize each response column over all trials to [0,1]. Use the goal-appropriate rule:*

Larger-the-better

$$x_i(j) = \frac{y_i(j) - miny(j)}{maxy(j) - miny(j)} \quad (3)$$

Smaller-the-better

$$x_i(j) = \frac{maxy(j) - y_i(j)}{maxy(j) - miny(j)} \quad (4)$$

where
$y_i(j)$ is the raw value of alternative 'i' under criterion 'j';
$miny(j)\ and\ maxy(j)$ - minimum and maximum value of criterion 'j' across all alternatives;
$x_i(j)$ - normalized value, mapped into [0,1].

Step 2: *Deviation sequence*

$$\Delta_i(j) = |1 - x_i(j)| \quad (5)$$

where $x_i(j)$ =normalized value of the i[th] alternative at the j[th] criterion.

Step 3: *Grey Relational Coefficient (GRC) is a measure that converts the deviation of an alternative from the ideal value into a standardized score between 0 and 1*

$$\xi_i(j) = \frac{\Delta_{min} + \rho\Delta_{max}}{\Delta_i(j) + \rho\Delta_{max}} \quad (6)$$

where $0 < \rho \leq 1$ is the distinguishing coefficient (commonly ρ=0.5); and Δ_{min} and Δ_{max} are the minimum and maximum of all $\Delta_i(j)$ across response.

Step 4: *Grey Relational Grade (GRG) is the average of all Grey Relational Coefficients* [21]

$$\gamma_i = \frac{1}{m}\sum_{j=1}^{m}\xi_i(j) \quad (7)$$

where:
γ_i - Grey Relational Grade (GRG) for alternative i;
m - number of criteria;
$\xi_i(j)$ - Grey Relational Coefficient (GRC).

5. TOPSIS TECHNIQUE

It is a nonparametric identification process that selects the optimal option among multiple options. This approach of vector measuring eliminates standard units associated with standard functions. The six-step TOPSIS methodology integrated the Five Output replies into a one consolidated output [22-23].

Step 1: *Decision Matrix*

Define the decision matrix with alternatives.

$$X = [x_{ij}], i = 1,2,\ldots,mj = 1,2,\ldots,n \quad (8)$$

where:
m - number of alternatives;
n- number of criteria;
x_{ij}- performance value of alternative $'i'$ under criterion $'j'$.

Step 2*: Normalize the Decision Matrix*

Convert the raw data into dimensionless values using vector normalization.

$$r_{ij} = \frac{x_{ij}}{\sqrt{\sum_{i=1}^{m} x_{ij}^2}} \text{ for } i = 1,2,\dots,m; j = 1,2,\dots,n \quad (9)$$

Step 3: *Weighted Normalized Matrix*

Multiply each normalized value by its corresponding weight $w_j = 0.4$

$$v_{ij} = w_j \cdot r_{ij} \quad (10)$$

Step 4: *Determine the Positive Ideal Solution (PIS) and Negative Ideal Solution (NIS)*

$$v_{ij}{}^{+} = \{v_1^+, v_2^+, \dots, v_n^+\} \quad (11)$$

$$v_{ij}{}^{-} = \{v_1^-, v_2^-, \dots, v_n^-\} \quad (12)$$

Step 5*: Calculate the Separation Measures*

Compute the Euclidean distance of each alternative from PIS and NIS

$$S_i^+ = \sqrt{\sum_{j=1}^{n} \left(v_{ij} - v_j^+\right)^2}$$
$$S_i^- = \sqrt{\sum_{j=1}^{n} \left(v_{ij} - v_j^-\right)^2} \quad (13)$$

Step 6*: Relative Closeness*

$$C_i = \frac{S_i^-}{S_i^+ + S_i^-}, 0 \le C_i \le 1 \quad (14)$$

6. ANFIS METHOD

The Adaptive Neuro-Fuzzy Inference System (ANFIS) employs a structured, five-layer network architecture. Each layer performs a specific transformation of the input data toward producing a crisp output:

Fuzzification Layer: *Nodes in this layer apply membership functions to crisp inputs, converting them into fuzzy membership values (equation 15).*

$$B_i^1 = \mu A_i(x_1), \text{ for } i = 1,2 \quad (15)$$

Implication Layer: *This layer computes the* firing strength *of each fuzzy rule by combining the membership values—typically using multiplication (equation (16).*

$$\mathrm{B_i^2} = w_\mathrm{i} = \mu \mathrm{A_i(y)} \mu \mathrm{B_i} - 2(\mathrm{y_2}), \text{ for i} = 1,2 \quad (16)$$

Normalization Layer: *Normalizes rule firing strengths by dividing each w_i by the sum of all rule strengths (equation 17).*

$$\mathrm{B_i^3} = \bar{N}_\mathrm{i} = \frac{N_i}{N_1 + N_2} \text{ for i} = 1,2 \quad (17)$$

Defuzzification layer: *Each normalized weight $\bar{N}_i$ is used to scale a linear consequent function of the inputs (equation 18).*

$$B_\mathrm{i}^4 = \bar{N}_i \mathrm{y_i} = \bar{N}_\mathrm{i}(\mathrm{p}_i \mathrm{Y} + \mathrm{q}_i \mathrm{Y} + \mathrm{r}_i), \text{ for i} = 1,2 \dots \quad (18)$$

Combination Layer: *The final output is the sum of all rule outputs equation (19).*

$$B_\mathrm{i}^5 = \sum_j (\bar{N}_i y_i) = \frac{\sum_i (N_i y_i)}{\sum_i N_i} \quad (19)$$

7. RESULTS AND DISCUSSION

7.1. Signal-to-noise Ratio Analysis

MINITAB statistical software was utilized to identify the most significant parameters and their contributions to the EDM process responses through signal-to-noise ratio analysis [22]. For MRR, the optimal conditions were observed at the parameters combination (Ip 1 - Ton2 - Toff3 - Vg1 - Fp1 - Tr3) of discharge current of 3 A, a pulse on time of 175 µs, a pulse off time of 90 µs, a gap voltage of 30 V, a flushing pressure of 0.4 MPa, and a tool rotation speed of 900 rpm (Fig. 2).

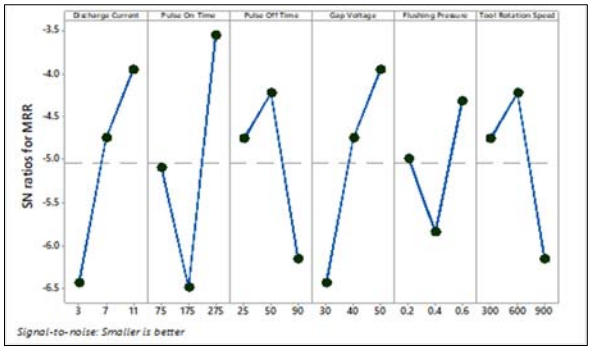

Fig. 2. SN ratio plot for MRR

In the case of tool wear rate (TWR), the best parameter combination was determined (Ip2 - Ton3 - Toff3 - Vg1 - Fp1 - Tr3) to be a discharge current of 7A, a pulse on time of 275µs, a pulse off time of 90µs, a gap voltage of 30 V, a flushing pressure of 0.2MPa, and a tool rotation speed of 900 rpm (Fig. 3).

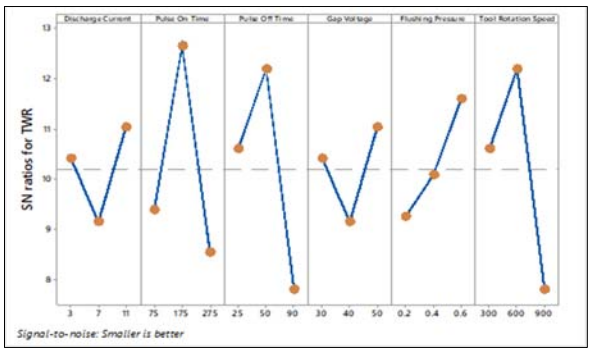

Fig. 3. SN ratio plot for TWR

For surface roughness, the optimal settings were found (Ip3 - Ton1 - Toff2 - Vg3 - Fp3 - Tr2) at a discharge current of 11A, a pulse on time of 75 µs, a pulse off time of 50µs, a gap voltage of 50 V, a flushing pressure of 0.6MPa, and a tool rotation speed of 600rpm (Fig. 4). Similarly, for the recast layer, the most favourable parameters were identified (Ip3 - Ton3 - Toff2 - Vg3 - Fp2 - Tr2) as a discharge current of 11A, a pulse on time of 275µs, a pulse off time of 50µs, a gap voltage of 50V, a flushing pressure of 0.4MPa, and a tool rotation speed of 600 rpm (Fig. 5).

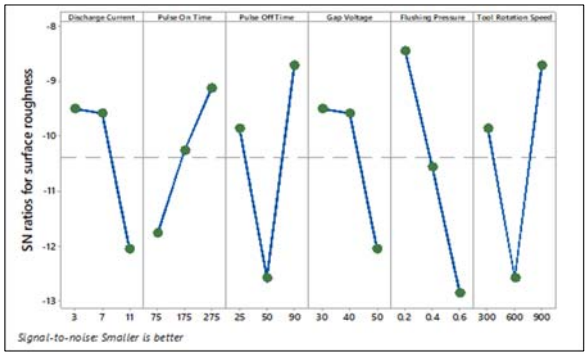

Fig. 4. SN ratio plot for surface roughness

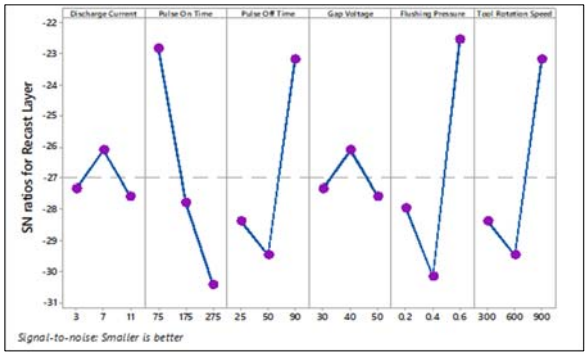

Fig. 5. SN ratio plot for recast layer

Lastly, the best parameter combination for microhardness was obtained (Ip3 - Ton1 - Toff1 - Vg3 - Fp2 - Tr1) at a discharge current of 11A, a pulse on time of 75µs, a pulse off time of 25µs, a gap voltage of 50 V, a flushing pressure of 0.4MPa, and a tool rotation speed of 300 rpm (Fig. 6).

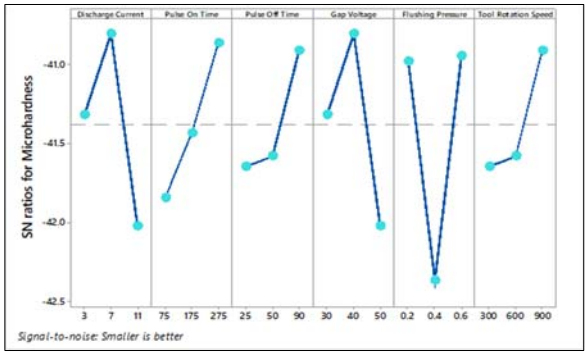

Fig. 6. SN ratio plot for micro hardness

From figure 7, the Pareto chart of standardized effects for MRR revealed that the most influential factor was the interaction between pulse off time and flushing pressure (CE), followed by the quadratic effect of pulse on time (BB), pulse on time (B), pulse off time (C), and tool rotation speed (F), all of which exceed the significance threshold line at $\alpha = 0.05$, indicating their strong contribution to material removal rate. Moderate effects were observed for interactions such as discharge current with pulse off time (AC), discharge current with flushing pressure (AE), and discharge current with tool speed (AF). In contrast, flushing pressure (E), discharge current squared (AA), and other minor interactions remain below the significance line, suggesting minimal impact. Overall, the analysis highlighted pulse on time, pulse off time, their quadratic terms, and their interactions with flushing pressure and tool rotation speed as the most critical parameters in determining MRR.

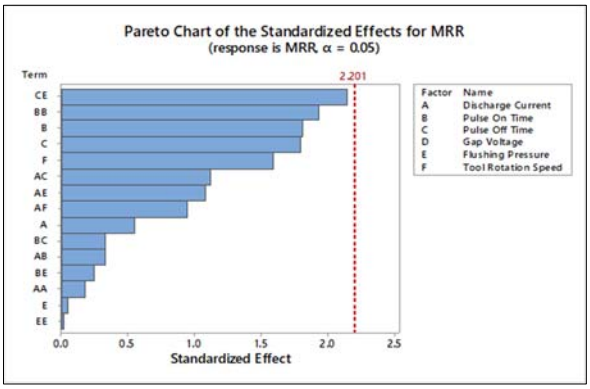

Fig. 7. Pareto chart for MRR

From figure 8, the Pareto chart of standardized effects for TWR indicated that the interaction between discharge current and pulse on time (AB) was the most influential factor, exceeding the significance threshold at $\alpha = 0.05$, and therefore played a dominant role in determining tool wear rate.

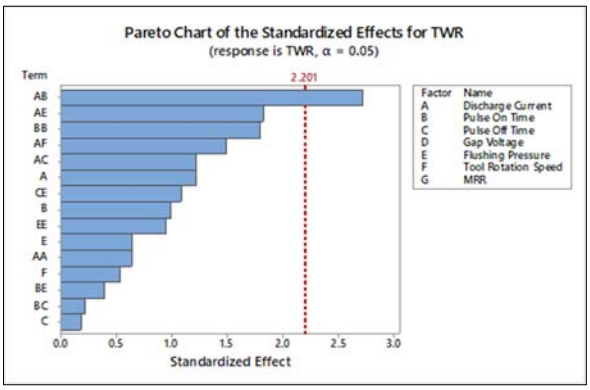

Fig. 8. Pareto chart for TWR

Other factors such as the interaction of discharge current with flushing pressure (AE), the quadratic effect of pulse on time (BB), and the interaction

between discharge current and tool rotation speed (AF), also showed considerable effects. Moderate contributions were observed from the interaction of discharge current with pulse off time (AC) and the main effect of discharge current (A), as well as from pulse on time (B) and the interaction between pulse off time and flushing pressure (CE).

From Figure 9, the Pareto chart of standardized effects for surface roughness showed that the interaction between pulse on time and pulse off time (BC) exhibits the highest influence, followed by flushing pressure (E) and the interaction of pulse on time with flushing pressure (BE). Moderate contributions are observed from pulse on time (B), its quadratic effect (BB), and flushing pressure squared (EE), along with discharge current (A) and its related interactions.

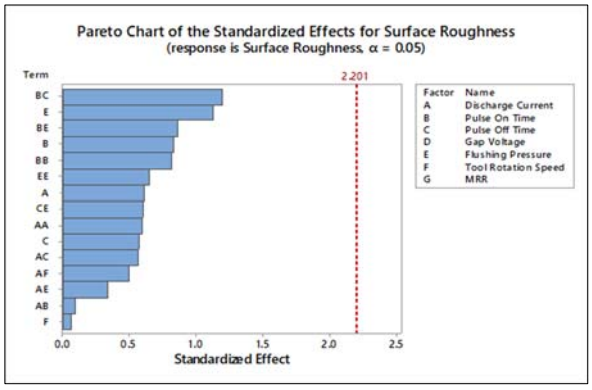

Fig. 9. Pareto chart for surface roughness

The Pareto chart showed that Pulse On Time (B) was the only statistically significant factor influencing the recast layer at the 95% confidence level, as its standardized effect exceeds the critical value of 2.201, while all other factors and interactions including flushing pressure (EE), the interaction between discharge current and pulse off time (AC), and others fall below the threshold. This indicates that adjusting pulse on time is the most effective way to control recast layer thickness, whereas the remaining factors have comparatively minor effects (Fig. 10).

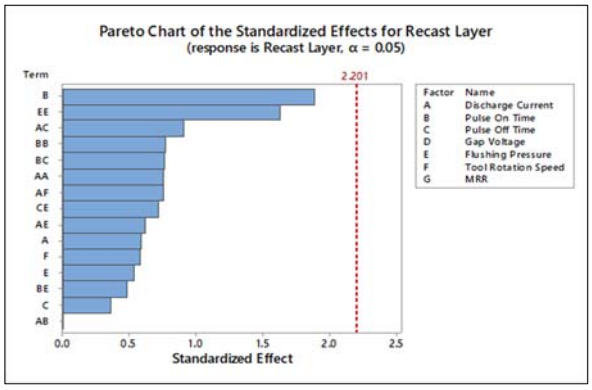

Fig. 10. Pareto chart for recast layer

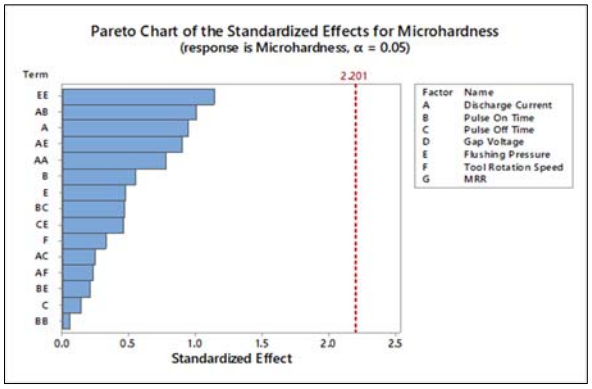

Fig. 11. Pareto chart for micro hardness

This Pareto chart of standardized effects for microhardness showed that EE (quadratic effect of flushing pressure), AB (interaction of discharge current and pulse on time), and A (discharge current), were most statistically significant factors, followed by AE and AA terms, while pulse on time (B), flushing pressure (E), and other interactions have comparatively smaller effects (Fig. 11).

7.2. GRA and Topsis Result

The Taguchi method has widely recognized for its simplicity and effectiveness in parameter optimization, but it was primarily suited for single-objective problems. To address the limitations of multi-objective optimization, researchers have increasingly combined the Taguchi approach with GRA and TOPSIS. These hybrid techniques transform multi-objective problems into equivalent single-objective problems, making optimization more practical and efficient. In GRA, normalization and deviation sequences were used to calculate the GRC, with the results of normalization and GRG presented in tables 4 and 5, respectively. A higher GRG value represents a superior quality response, and figure 12 highlighted the optimal parameter settings for improving MRR and MHS, along with the contribution of each factor.

Based on GRA method, the optimal EDM parameters for machining aluminum alloy were identified as 11 A discharge current, 75 µs pulse on time, 25 µs pulse off time, 50 V gap voltage, 0.4 MPa flushing pressure, and 600 rpm tool rotation speed, yielding the best overall performance by increasing MRR and microhardness while decreasing TWR, surface roughness, and recast layer and surface roughness. In contrast, using TOPSIS approach, the normalization results is shown in table 6 and (PIS), NIS, and Closeness Coefficient is presented in table 7. From figure 17, it was determined an alternative optimal setting of 7A discharge current, 175µs pulse on time, 90 µs pulse off time, 40V gap voltage, 0.5MPa flushing pressure, and 900 rpm tool rotation speed, which also delivered enhanced machining performance by improving MRR and microhardness and reducing TWR, surface roughness, and recast layer thickness.

Table 4. Normalization Responses for GRA

Run	MRR [g/min]	Microhardness [HV]	TWR [g/min]	Surface roughness, Ra [µm]	Recast layer [µm]
1	0.3728	0.2366	0.487	0.3964	0.3224
2	0.9798	0.0749	0.4034	0.0662	0.6538
3	0.7494	0.3021	0.9871	0.9155	0.9568
4	0.6089	0.1644	0.3871	0.8059	0.6763
5	0.1427	0.9866	0.8545	0.9596	0.6601
6	0.1426	0.8556	0.9672	0.6741	0.2017
7	0.0395	0.6698	0.0222	0.6095	0.3061
8	0.8907	0.9238	0.0043	0.7291	0.0231
9	0.6115	0.8516	0.1724	0.1611	0.4936
10	0.7242	0.1912	0.7112	0.6421	0.8932
11	0	0.9465	0.9323	0.7194	0.2204
12	1	0.5682	0.3052	0.4526	0.1664
13	0.8552	0.8556	0.5662	0.862	0.3925
14	0.202	0.9505	0.9063	0.1881	0.1549
15	0.1698	0.3316	0.5073	0.9296	0.4692
16	0.1715	0.1096	1	0	0.4363
17	0.2988	0.2353	0.0644	0.2187	0.5443
18	0.5311	0.4492	0.7602	0.8032	1
19	0.4333	0.8663	0.3284	1	0.9064
20	0.2851	0.9131	0.7034	0.1746	0.9933
21	0.6228	0	0.4806	0.2853	0.3074
22	0.1252	0.5388	0.4522	0.2628	0.6724
23	0.286	0.4385	0.8392	0.2197	0.4523
24	0.3642	0.2299	0	0.9301	0
25	0.4587	0.1203	0.2079	0.6403	0.7462
26	0.8054	0.3529	0.0322	0.8875	0.5637
27	0.1886	1	0.08	0.1261	0.1723

Table 5. Grey relational coefficient and GRG results

Run	Grey relational coefficient (GRC)					GRG
	MRR [g/min]	Microhardness [HV]	TWR [g/min]	Surface roughness, Ra [µm]	Recast layer [µm]	
1	0.4436	0.3958	0.4936	0.4531	0.4246	0.4421
2	0.9611	0.3508	0.4559	0.3487	0.5909	0.5415
3	0.6661	0.4174	0.9749	0.8554	0.9204	0.7669
4	0.5611	0.3744	0.4493	0.7203	0.607	0.5424
5	0.3684	0.974	0.7746	0.9252	0.5953	0.7275
6	0.3684	0.7759	0.9385	0.6054	0.3851	0.6147
7	0.3423	0.6023	0.3383	0.5615	0.4188	0.4526
8	0.8207	0.8677	0.3343	0.6486	0.3385	0.602
9	0.5628	0.7711	0.3766	0.3734	0.4968	0.5162
10	0.6445	0.382	0.6338	0.5828	0.824	0.6134
11	0.3333	0.9034	0.8808	0.6405	0.3907	0.6297
12	1	0.5366	0.4185	0.4774	0.3749	0.5615
13	0.7754	0.7759	0.5354	0.7837	0.4515	0.6644
14	0.3852	0.91	0.8422	0.3811	0.3717	0.578
15	0.3759	0.4279	0.5037	0.8766	0.485	0.5338
16	0.3764	0.3596	1	0.3333	0.4701	0.5079
17	0.4162	0.3953	0.3483	0.3902	0.5232	0.4147
18	0.516	0.4758	0.6758	0.7175	1	0.677
19	0.4687	0.789	0.4268	1	0.8424	0.7054

Run	Grey relational coefficient (GRC)					GRG
	MRR [g/min]	Microhardness [HV]	TWR [g/min]	Surface roughness, Ra [μm]	Recast layer [μm]	
20	0.4115	0.8519	0.6277	0.3772	0.9867	0.651
21	0.57	0.3333	0.4905	0.4116	0.4193	0.4449
22	0.3637	0.5202	0.4772	0.4041	0.6042	0.4739
23	0.4119	0.471	0.7567	0.3905	0.4772	0.5015
24	0.4402	0.3937	0.3333	0.8774	0.3333	0.4756
25	0.4802	0.3624	0.387	0.5816	0.6633	0.4949
26	0.7198	0.4359	0.3406	0.8163	0.534	0.5693
27	0.3813	1	0.3521	0.3639	0.3766	0.4948

Table 6. Normalization for TOPSIS

Run	MRR [g/min]	Microhardness [HV]	TWR [g/min]	Surface roughness, Ra [μm]	Recast layer [μm]
1	0.13992	0.15454	0.16541	0.20905	0.2235
2	0.34404	0.13552	0.18997	0.31859	0.12142
3	0.26656	0.16224	0.01856	0.03681	0.02811
4	0.21932	0.14605	0.19473	0.07318	0.1145
5	0.0625	0.24274	0.05751	0.02218	0.11947
6	0.0625	0.22733	0.0244	0.11689	0.26066
7	0.02781	0.20548	0.30188	0.13832	0.22853
8	0.31409	0.23535	0.30712	0.09864	0.31569
9	0.22019	0.22686	0.25777	0.28712	0.17078
10	0.25808	0.1492	0.09959	0.12752	0.04769
11	0.01453	0.23802	0.03465	0.10188	0.25492
12	0.35084	0.19353	0.21878	0.19038	0.27155
13	0.30214	0.22733	0.14216	0.05455	0.2019
14	0.08246	0.23849	0.04229	0.27815	0.2751
15	0.07164	0.1657	0.15944	0.03212	0.17829
16	0.07221	0.13961	0.01478	0.34057	0.18841
17	0.11501	0.15438	0.28948	0.26801	0.15515
18	0.19314	0.17954	0.08521	0.07408	0.01479
19	0.16025	0.22859	0.21198	0.00876	0.04361
20	0.1104	0.23409	0.10186	0.28264	0.01686
21	0.22399	0.12671	0.16727	0.2459	0.22812
22	0.05665	0.19007	0.17562	0.25338	0.11568
23	0.11073	0.17828	0.062	0.26767	0.1835
24	0.13702	0.15375	0.3084	0.03195	0.32279
25	0.1688	0.14086	0.24735	0.12811	0.09296
26	0.2854	0.16822	0.29894	0.04609	0.14918
27	0.07797	0.24431	0.28491	0.29872	0.26971

Table 7. Closeness Coefficient in TOPSIS

Run	S+ (to ideal best)	S- (to ideal worst)	TOPSIS CC
1	0.07973	0.05064	0.38843
2	0.07744	0.08092	0.51099
3	0.02435	0.11452	0.82469
4	0.0542	0.08249	0.6035
5	0.062	0.09411	0.60284
6	0.07891	0.07667	0.49281
7	0.10015	0.04742	0.32133
8	0.08614	0.08003	0.48161
9	0.08443	0.05687	0.40247

Run	S+ (to ideal best)	S- (to ideal worst)	TOPSIS CC
10	0.04001	0.09476	0.7031
11	0.08482	0.07718	0.47639
12	0.07566	0.07766	0.50654
13	0.04732	0.09315	0.6631
14	0.09234	0.06135	0.39919
15	0.07276	0.07563	0.50968
16	0.09567	0.06565	0.40696
17	0.09509	0.04223	0.30753
18	0.03914	0.10008	0.71887
19	0.05524	0.0957	0.63401
20	0.07497	0.08008	0.51649
21	0.07872	0.05717	0.42073
22	0.08611	0.05437	0.38704
23	0.07993	0.0624	0.43841
24	0.09706	0.06663	0.40704
25	0.06878	0.07091	0.50759
26	0.06641	0.08765	0.56891
27	0.1089	0.03031	0.21775

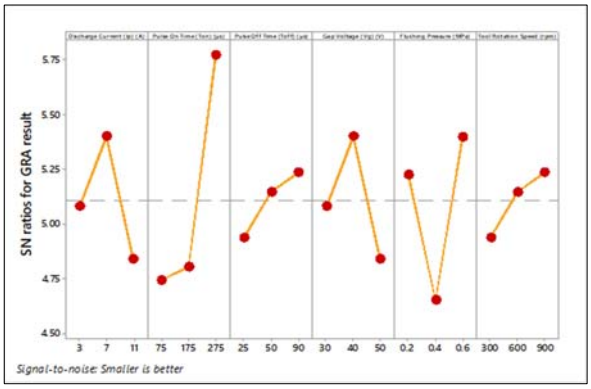

Fig. 12. SN ratio plots for GRA result

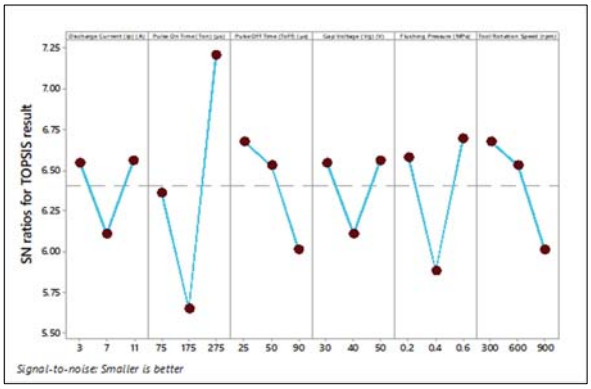

Fig. 13. SN ratio plots for TOPSIS result

7.3. Prediction of the Accuracy of Data with ANFIS model

To evaluate the performance of the ANFIS model, the model was developed by incorporating six significant parameters identified through Output Responses (Fig.14). The fuzzy logic system utilized a rule base consisting of six inputs and FIVE outputs.

According to six inputs, $3^6 = 729$ rules are theoretically possible but this rule base containing 27 logic rules, was trained using a Neural Network for the prediction of output response accuracy. For example, in Experiment no: 17, with inputs of Discharge Current of 11A, Pulse On Time of 275µs, Pulse Off Time of 50µs, Gap Voltage of 50V, Flushing Pressure of 0.6 MPa and Tool Rotation Speed of 600 rpm, the predicted ANFIS model value for TWR is 0.728, as presentedin figure 15.

Figures 16 to 20 illustrate the comparison between the experimental results and the ANFIS-predicted values for all five output responses. Those figures clearly showing that the prediction accuracy is very close to unity, which highlights the strong correlation and reliability of the developed model. The coefficient of determination (R2) values obtained for different responses further validate the robustness of the prediction: MRR achieved an accuracy of 0.923, TWR reached 0.870**,** Surface Roughness recorded the highest accuracy of 0.980**,** Recast Layer attained 0.974**,** and Microhardness reached 0.932. Such high R2 values across all machining characteristics demonstrate that ANFIS can capture the complex nonlinear relationships between process parameters and responses with remarkable precision. These findings confirm that ANFIS is a powerful and reliable modeling tool for optimizing machining performance, offering both predictive accuracy and practical applicability in real-world manufacturing processes. GRA and TOPSIS optimal parameters were inserted in the ANFIS model to predict the output responses for GRA and TOPSIS methods.

Figures 16 to 20 show the experimental vs ANFIS predicted data for all output responses. From the observations, MRR, RL and SR predicted values are very close to experimental values but TWR and MH predicted values are slight fluctuations or are deviated from experimental values. This comparison indicates the model's effectiveness and reliability in predicting machining performance and quality characteristics.

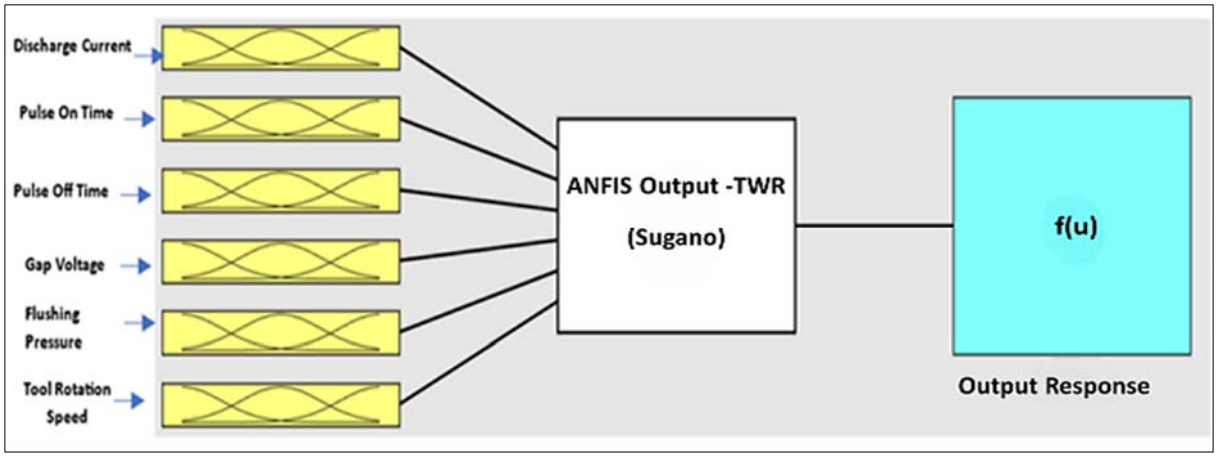

Fig. 14. FIS model inputs and output (TWR)

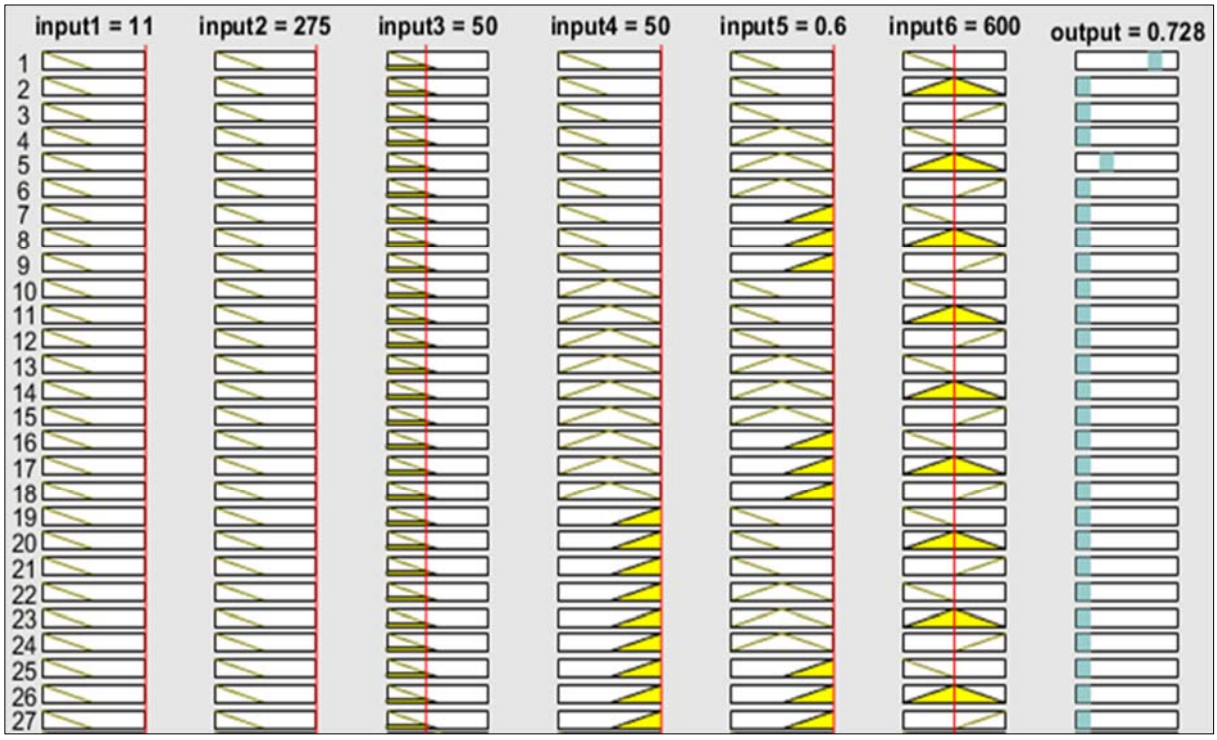

Fig. 15. Rule base for fuzzy logic inference using a neural network in ANFIS with 6 inputs and 1 output for TWR

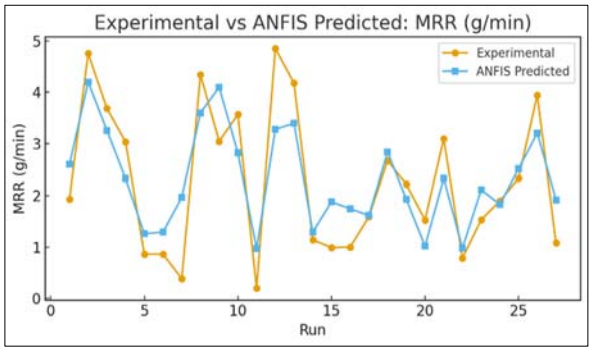

Fig. 16. Experimental vs. ANFIS predicted data for MRR

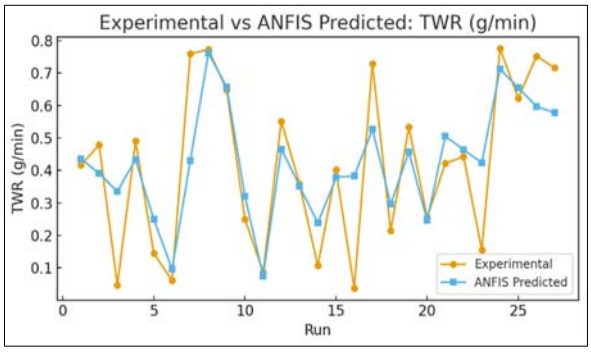

Fig. 17. Experimental vs ANFIS predicted data for TWR

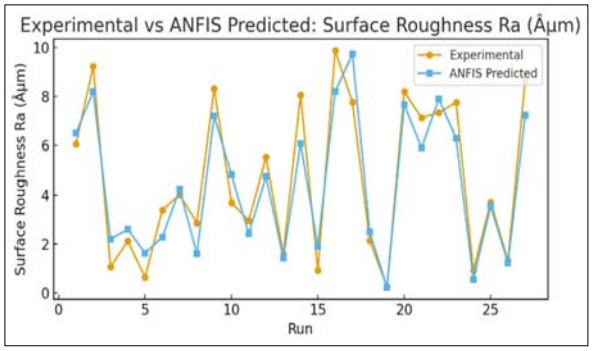

Fig. 18. Experimental vs ANFIS predicted data for surface roughness

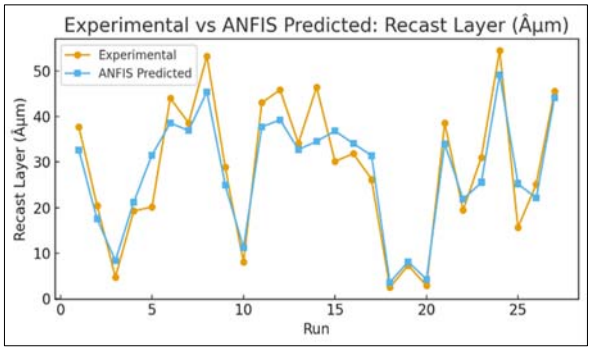

Fig. 19. Experimental vs ANFIS predicted data for recast layer

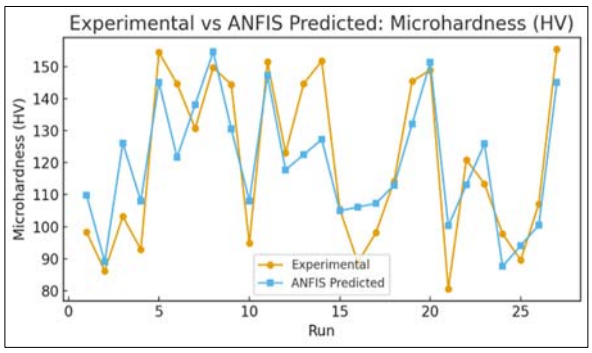

Fig. 20. Experimental vs ANFIS predicted data for micro hardness

Comparing the optimization results of GRA and TOPSIS, it becomes evident that each method emphasizes different machining priorities (Table 8). For MRR, GRA produced a significantly higher value of 4.76 g/min compared with TOPSIS (0.78 g/min) value. This difference arises because GRA favors higher discharge current and shorter off-time, which means more aggressive energy is delivered to the workpiece in a shorter interval, leading to faster melting and removal of material. For TWR, both techniques were relatively close, with GRA at 0.478 g/min and TOPSIS slightly better at 0.442 g/min. The marginal improvement under TOPSIS is attributed to lower energy input per cycle, which reduces thermal and mechanical stresses on the electrode and thereby prolongs tool life. For SRS, TOPSIS outperforms GRA, yielding a smoother finish of 7.34 µm compared to 9.23 µm. This improvement is a result of the milder discharge conditions in TOPSIS that allow for a more controlled melting–solidification process, minimizing surface pitting and irregularities.

Similarly, the RLR is slightly reduced under TOPSIS (19.6 µm) compared to GRA (20.5 µm), which indicates that controlled flushing and reduced discharge energy prevent excessive molten material from resolidifying on the machined surface. Finally, for MHS, TOPSIS exhibits a distinct advantage, producing a much higher value of 120.9 HV against GRA's 86.2 HV. This significant increase suggests that the slower material removal and controlled discharge conditions in TOPSIS promote beneficial microstructural changes, rapid solidification, grain refinement and also enhance hardness.

Table 8. Comparison Results of GRA and TOPSIS through ANFIS

Technique	Input parameters						Output parameters				
	Ip [A]	Ton [µs]	Toff [µs]	Vg [V]	FP [MPa]	N [rpm]	MRR [g/min]	TWR [g/min]	SRS [µm]	RLR [µm]	MHS [HV]
GRA	11	75	25	50	0.4	600	4.76	0.478	9.23	20.5	86.2
TOPSIS	7	175	90	40	0.5	900	0.78	0.442	7.34	19.6	120.9

8. CONCLUSIONS

This present work has been carried out based on datasets collected from earlier experimental work, the effects of discharge current, pulse-on/off times, gap voltage, flushing pressure, and tool rotation speed on machining responses were systematically evaluated. The output responses MRR, TWR, SRS, RLR, and MHS were optimized through GRA and TOPSIS methods. The conclusion were made based on the results below:

- According to SN ratio results, the optimal conditions were observed for MRR, at the parameters combination (Ip1 - Ton 2 - Toff 3 - Vg1 - Fp1 - Tr3) of discharge current of 3A, a pulse on time of 175µs, a pulse off time of 90µs, a gap

voltage of 30V, a flushing pressure of 0.4MPa, and a tool rotation speed of 900rpm. The Pareto chart of standardized effects for MRR revealed that the most influential factor was the interaction between pulse off time and flushing pressure, followed by other parameters.

- Based on GRA method, the optimal EDM parameters for machining aluminum alloy were identified as 11 A discharge current, 75 µs pulse on time, 25 µs pulse off time, 50 V gap voltage, 0.4 MPa flushing pressure, and 600 rpm tool rotation speed, yielding the best overall performance. For TOPSIS method, optimal setting is for using 7 A discharge current, 175 µs pulse on time, 90 µs pulse off time, 40 V gap voltage, 0.5 MPa flushing pressure, and 900 rpm tool rotation speed, which also delivered enhanced machining performance.
- The comparative results highlight two distinct optimization directions. GRA emphasized higher productivity, achieving the best MRR of 4.76 g/min under higher current and shorter pulse-off conditions, though at the expense of surface smoothness and recast control. In contrast, TOPSIS identified a more balanced set of parameters that produced smoother surfaces (7.34 µm), thinner recast layers (19.6 µm), slightly lower TWR (0.442 g/min), and notably higher microhardness (120.9 HV). These findings suggest that GRA is more effective when rapid stock removal is prioritized, while TOPSIS offers superior outcomes when surface integrity and mechanical properties are the main objectives.
- The integration of optimized results into the ANFIS model further demonstrated accurate prediction of machining responses, validating its potential for intelligent process control. This dual optimization approach thus provides manufacturers with flexibility to choose between productivity and quality priorities, paving the way for more adaptive and application-specific EDM strategies.

ABBREVIATIONS

Ip - Discharge Current
Fp - Flushing Pressure
GRA - Grey Relational Analysis
MRR - Material Removal Rate
MHS - Micro Hardness
RLR - Recast Layer
SRS - Surface Roughness
Ton - Pulse On Time
Toff - Pulse Off Time
TOPSIS - Technique for Order Preference by Similarity to Ideal Solution
Tr - Tool Rotation Speed
TWR - Tool Wear Rate
Vg - Gap Voltage

REFERENCES

[1] **Kumar J.**, **Sharma S.**, **Singh J.**, **Singh S.**, **Singh G.**, *Optimization of Wire-EDM Process Parameters for Al-Mg-0.6Si-0.35Fe/15%RHA/5%Cu Hybrid Metal Matrix Composite Using TOPSIS: Processing and Characterizations*, Journal of Manufacturing and Materials Processing, 2022, vol. 6, iss. 6, p. 150.

[2] **Nas E.**, **Kara F.**, *Optimization of EDM Machinability of Hastelloy C22 Super Alloys*, Machines, 2022, vol. 10, iss. 12, p. 1131.

[3] **Chen S. L.**, **Yan B. H.**, **Huang F. Y.**, *Influence of kerosene and distilled water as dielectrics on the electric discharge machining characteristics of Ti-6Al-4V*, Journal of Materials Processing Technology, 1999, vol. 87, iss. 1-3, pp. 107-111.

[4] **Singh V.**, **Sharma A. K.**, **Goyal A.**, **Saxena K. Kumar**, **Negi P.**, **Rao P. C. S.**, *Electric discharge machining performance measures and optimisation: a review*, Advances in Materials and Processing Technologies, 2024, vol. 10, iss. 2, pp. 517-530.

[5] **Chen Y.**, **Hu S.**, **Li A.**, **Cao Y.**, **Zhao Y.**, **Ming W.**, *Parameters Optimization of Electrical Discharge Machining Process Using Swarm Intelligence: A Review*, Metals, 2023, vol. 13, iss. 5, p. 839.

[6] **Mariya Louis D.**, **Manivel S.**, **Seeniappan K.**, **L N.**, *Multiresponse optimization and network-based prediction modelling for the WEDM of AM60B biomedical material*, Proceedings of the Institution of Mechanical Engineers, Part C: Journal of Mechanical Engineering Science, 2024, vol. 238, iss. 20, pp. 10045-10066.

[7] **Mohankumar V.** et al., *Process parameters optimization of EDM for hybrid aluminum MMC using hybrid optimization technique*, Heliyon, 2024, vol. 10, iss. 15, p. e35555.

[8] **Suraya L.**, et al., *The Effect of EDM Die-Sinking Parameters on Machining Characteristics in Aluminum Alloy Machining*, Applied Mechanics and Materials, 2015, vol. 761, pp. 303-307.

[9] **Dave S.**, et al., *Optimization of EDM Drilling Parameters for Aluminum 2024 Alloy Using Response Surface Methodology and Genetic Algorithm*, Key Engineering Materials, 2016, vol. 706, pp. 3-8.

[10] **Bańkowski D.**, **Młynarczyk P.**, *Influence of EDM Process Parameters on the Surface Finish of Alnico Alloys*, Materials, 2022, vol. 15, iss. 20, p. 7277.

[11] **Lakshmaiya N.**, **Chukka N. D. K. R.**, **Kaliappan S.**, **Balaji V.**, **Ross N. S.**, **Maranan R.**, *An integrated Artificial neural network technique to optimize the various parameters of Pineapple/SiO2/epoxy-based nanocomposites under NaOH treatment*, Results in Engineering, 2025, vol. 26, p. 104737.

[12] **Jagdale M.**, **Ambhore N.**, **Chaudhari R.**, **Kulkarni A.**, **Abdullah M.**, *Experimental investigation of process parameters in Wire-EDM of Ti-6Al-4V*, Scientific Reports, 2025, vol. 15, iss. 1, p. 5652.

[13] **Ghazi S. K.**, **Abdullah M. A.**, **Abdulridha H. H.**, *Investigating the Impact of EDM Parameters on Surface Roughness and Electrode Wear Rate in 7024 Aluminum Alloy*, Engineering, Technology & Applied Science Research, 2025, vol. 15, iss. 1, pp. 19401-19407.

[14] **Dewangan S.**, **Chattopadhyaya S.**, **Hloch S.**, *Investigation into Coal Fragmentation Analysis by Using Conical Pick*, Procedia Materials Science, 2014, vol. 5, pp. 2411-2417.

[15] **G. K. M. R.**, **R. G.**, **H. R. D.**, **S. R. M.**, *Development of hybrid model and optimization of surface roughness in electric discharge machining using artificial neural networks and genetic algorithm*, Journal of Materials Processing Technology, 2009, vol. 209, iss. 3, pp. 1512-1520.

[16] **Kalla D.**, **Sheikh-Ahmad J.**, **Twomey J.**, *Prediction of cutting forces in helical end milling fiber reinforced polymers*, International Journal of Machine Tools and Manufacture, 2010, vol. 50, iss. 10, pp. 882-891.

[17] **Karpat Y.**, **Özel T.**, *Mechanics of high speed cutting with curvilinear edge tools*, International Journal of Machine Tools and Manufacture, 2008, vol. 48, iss. 2, pp. 195-208.

[18] **Sulaiman O.**, **Hashim R.**, **Subari K.**, **Liang C. K.**, *Effect of sanding on surface roughness of rubberwood*, Journal of Materials Processing Technology, 2009, vol. 209, iss. 8, pp. 3949-3955.

[19] **Kumar S.**, **Singh R.**, **Singh T. P.**, **Sethi B. L.**, *Surface modification by electrical discharge machining: A review*, Journal of Materials Processing Technology, 2009, vol. 209, iss. 8, pp. 3675-3687.

[20] **Sivasundar V.**, et al., *Predicting Wear Performance of Al6063 Hybrid Composites Reinforced With Multi-Ceramic Particles Using Experimental and ANFIS Approaches*, Engineering Reports, 2025, vol. 7, iss. 8, e70359.
[21] **Chen H.-C.**, **Wisnujati A.**, **Mudjijana**, **Widodo A. M.**, **Lung C.-W.**, *Grey Relational Analysis and Grey Prediction Model (1, 6) Approach for Analyzing the Electrode Distance and Mechanical Properties of Tandem MIG Welding Distortion*, Materials, 2023, vol. 16, iss. 4, p. 1390.
[22] **Vijayakumar S.**, *Optimization of Friction Stir Welding Parameters for Dissimilar Aluminium Alloys Using RSM-GRA and RSM-TOPSIS: Towards Sustainable Manufacturing in Industry 4.0*, Results in Engineering, 2025, p. 107054.
[23] **Sriram D.**, et al., *Microstructure, mechanical properties of dissimilar friction stir welded AA6063/AA5052 alloys, and optimization of process parameters using Box Behnken-TOPSIS approach*, Kovove Materialy (Metalic Materials), 2024, vol. 62, iss. 6, pp. 363-375.